



UNIVERSITÀ DI PISA

SOCIAL NETWORK ANALYSIS  
A.A. 2017/2018

# Cambridge Analytica and Facebook: The Scandal and the Fallout on Twitter

Gianmarco Ricciarelli 555396  
Stefano Carpita 304902

*Data drives all we do.*

Cambridge Analytica main slogan.

*Rules don't matter for them.  
For them, this is a war, and it's all fair.*

Christopher Wylie,  
former datascientist at Cambridge Analytica, about its leaders.

# Contents

<b>1</b>	<b>The case story</b>	<b>1</b>
<b>2</b>	<b>Building the network</b>	<b>2</b>
<b>3</b>	<b>Network properties</b>	<b>3</b>
3.1	Degree distribution . . . . .	3
3.1.1	Random graphs . . . . .	4
3.2	Path analysis . . . . .	6
3.3	Hubs analysis . . . . .	8
<b>4</b>	<b>Network dynamics</b>	<b>10</b>
<b>5</b>	<b>Communities discovery</b>	<b>11</b>
5.1	K-Clique . . . . .	11
5.2	Label Propagation . . . . .	11
5.3	Louvain . . . . .	11
5.4	Girvan-Newman . . . . .	12
5.5	Demon . . . . .	12
5.6	Comparisons . . . . .	12
<b>6</b>	<b>Spreading</b>	<b>14</b>
6.1	Which model for news spreading? . . . . .	14
6.2	The New York Times vs La Repubblica . . . . .	14
6.3	SI model . . . . .	15
6.4	SIS model . . . . .	16
6.5	SIR model . . . . .	16
6.6	Threshold model . . . . .	17
<b>7</b>	<b>Summary</b>	<b>19</b>

# 1 | The case story

On Saturday 17 of March 2018, the newspapers The Observer and The New York Times broke reports on how the consulting firm Cambridge Analytica harvested private information from the Facebook profiles of more than 50 million users without their permission, making it one of the largest data leaks in the social network's history. [1]. REF OBSERVER

The whistleblower Christopher Wylie, datascientist and former director of research at Cambridge Analytica revealed... Cambridge Analytica described itself as a company providing consumer research, targeted advertising and other data-related services to both political and corporate clients.

What, Where, Who, Why, Where ?

Timeline da sistemare: [2]

- March 17, 2018: The Observer and The New York Times publish joint reports on data harvesting by Cambridge Analytica. UK Information Commissioner Elizabeth Denham issues statement that they are "investigating circumstances in which Facebook data may have been illegally acquired and used." Politicians in US and UK call for investigation.
- March 19, 2018: Channel 4 News publishes part 1 of their undercover investigation into Cambridge Analytica. Facebook sends investigators to Cambridge Analytica's offices. UK Information Commissioner orders them to stand down.
- March 20, 2018: Channel 4 News publishes part 2 of their undercover investigation into Cambridge Analytica, where they boast about getting Donald Trump elected. British MP Damian Collins calls on Facebook to present oral evidence on Cambridge Analytica. Facebook agrees to send former operations manager Sandy Parakilas. Facebook holds internal Q&A with attorney Paul Grewal to discuss the crisis, but CEO Mark Zuckerberg and COO Sheryl Sandberg do not attend. Cambridge Analytica suspends CEO Alexander Nix. Facebook demands to inspect Christopher Wylie's phone. FTC opens investigation into Facebook.
- to be continued...

## 2 | Building the network

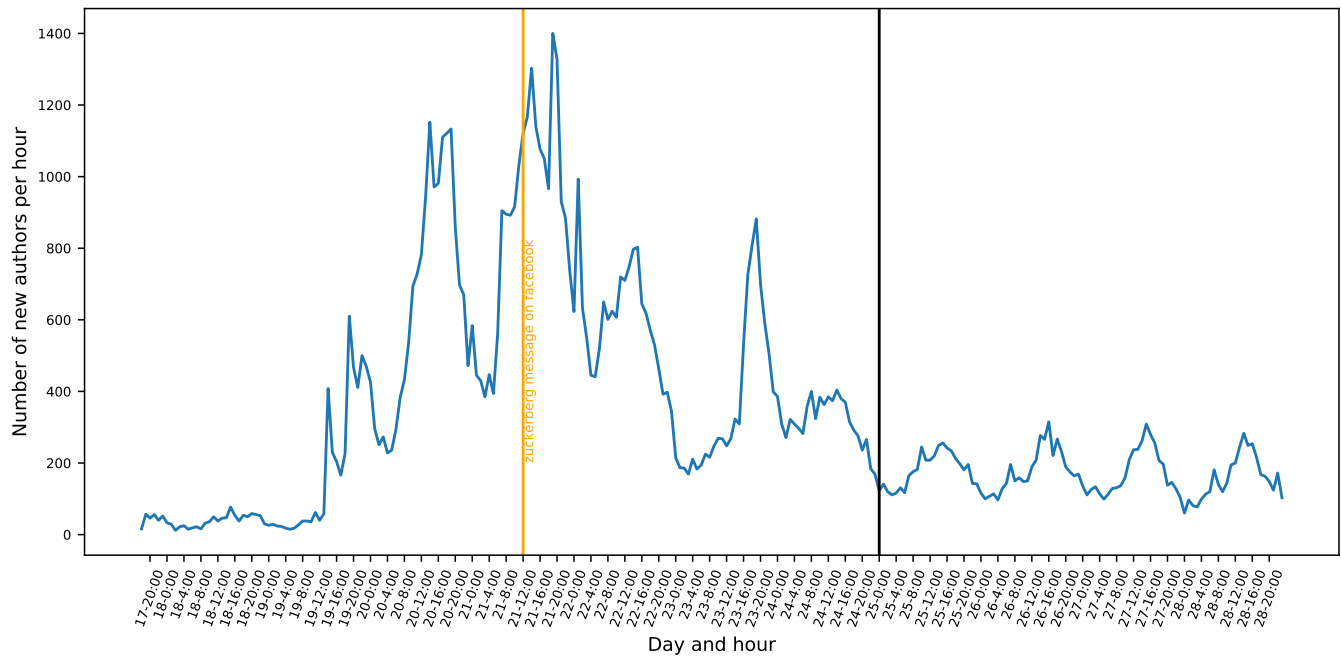


Figure 2.1: New authors time history

# 3 | Network properties

## 3.1 Degree distribution

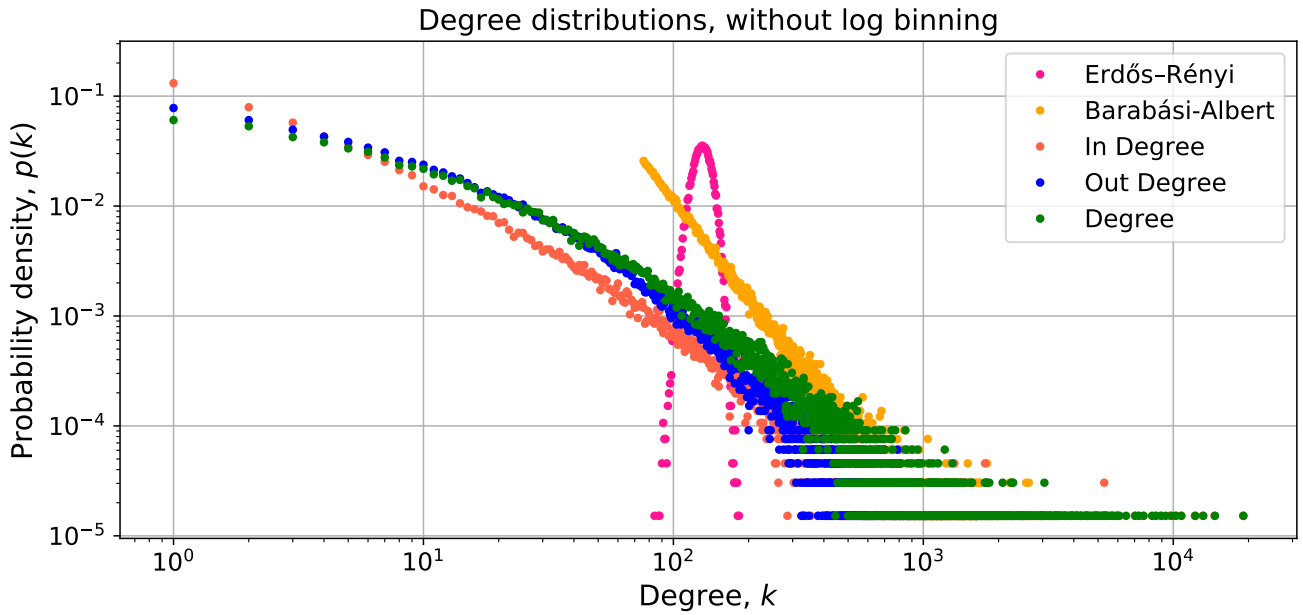


Figure 3.1: New authors time history

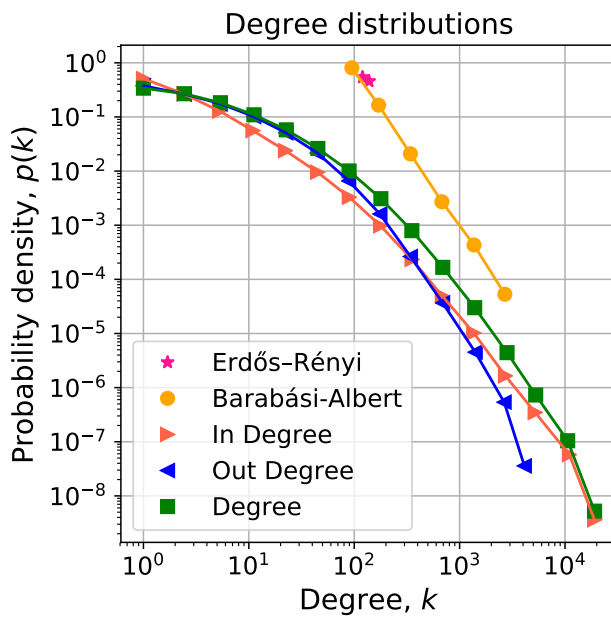


Figure 3.2

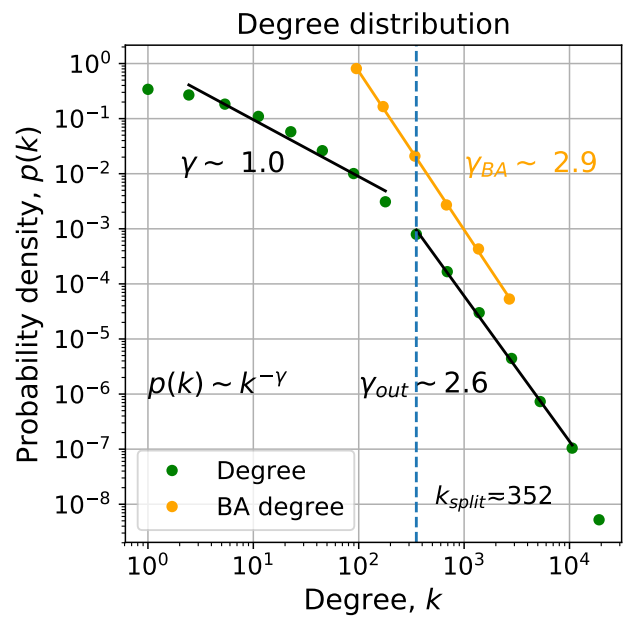


Figure 3.3

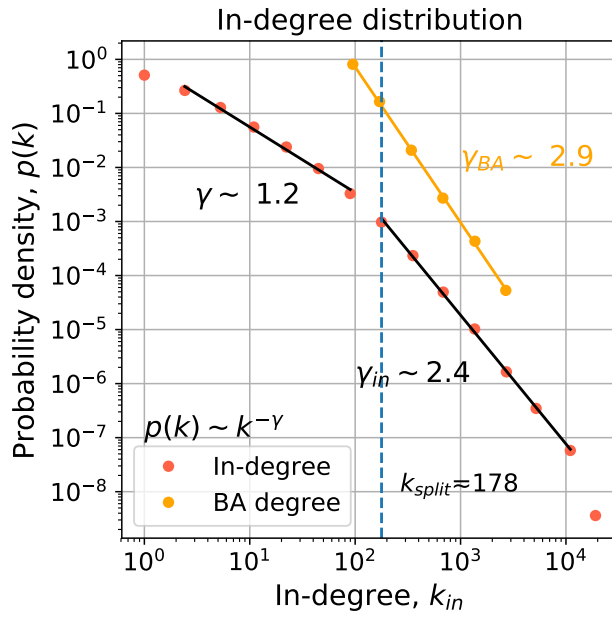


Figure 3.4

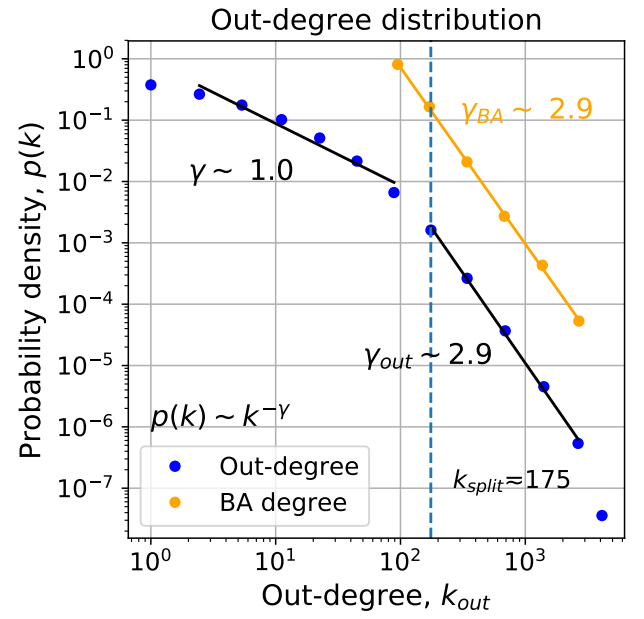


Figure 3.5

### 3.1.1 Random graphs

In order to generate an Erdos-Renyi random network we have chosen a “linking probability”  $p$  using the average degree of the original undirected network, by using eq. 3.1.

$$p_{ER} \approx \frac{\langle k \rangle}{N} = \frac{57}{65729} \approx 0.001 \quad (3.1)$$

Each new node of the random network generated with the Barabasi-Albert model has been attached to the other nodes with a number of links  $m$  equal to the average degree of the original network, considered undirected:

$$m = 2 \langle k \rangle = 76 \quad (3.2)$$

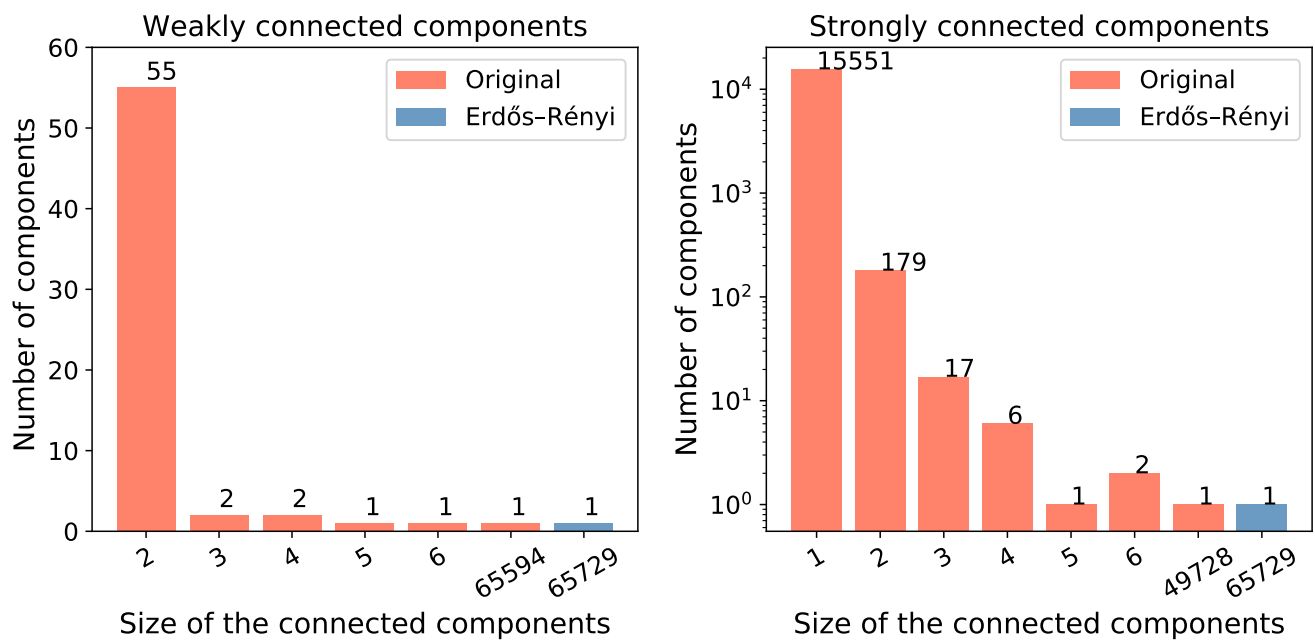


Figure 3.6: Connect components

## 3.2 Path analysis

In order to exactly estimate the average path length  $\langle d \rangle$  it would be necessary to compute all the node-node distances of the network. These procedure results infeasible with the computation resources available, as shown in Fig. 3.10. In real networks the path length distribution is quite close to a normal distribution, as shown in [3]. The average path length has then been estimated statistically, random sampling a number  $n$  of node pairs, sufficient to achieve a narrow confidence interval for the mean. The assumption of normality of the distribution it is strong, but not necessary. The convergence of the computed mean to the expected value is guaranteed by the central limit theorem with the assumptions that the distances are independent, identically distributed, and with finite variance. The average path length has been estimated by the average of the distances  $D_i$  for each sampled node pair, and computing its standard deviation:

$$\langle d \rangle = \frac{\sum D_i}{n}, \quad \sigma(\langle d \rangle) = \frac{s}{\sqrt{n}} \quad (3.3)$$

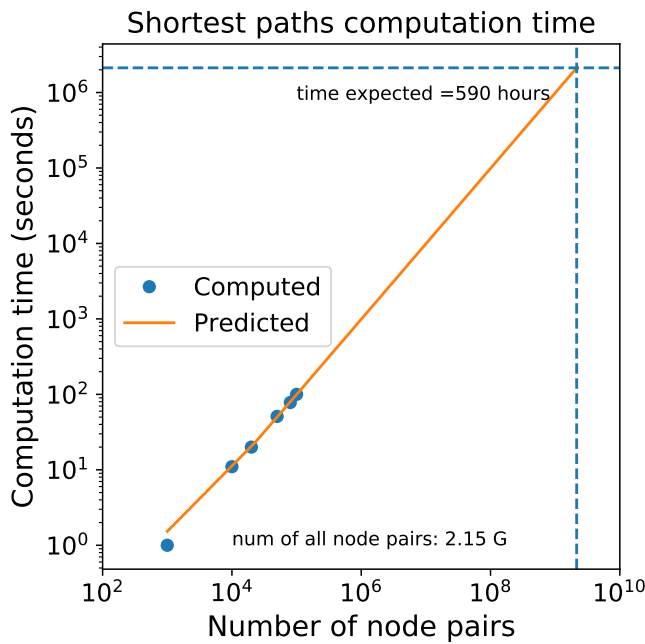


Figure 3.7: Shortest paths computation time by number of pairs

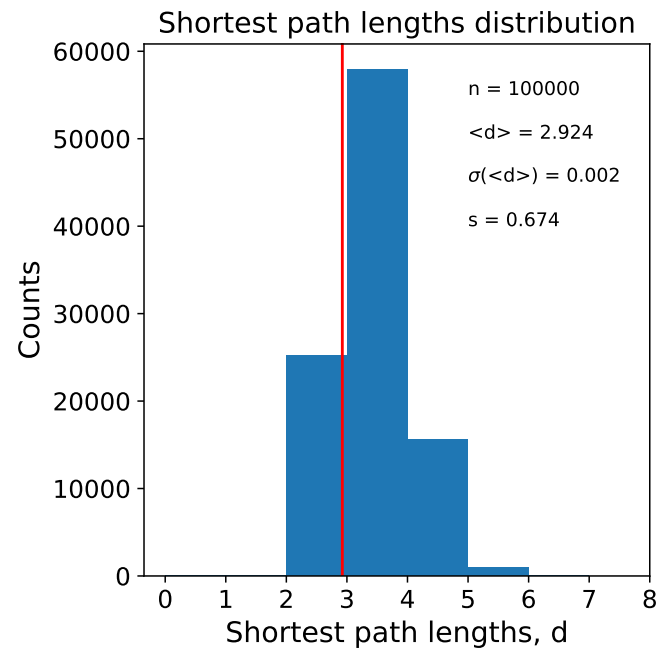


Figure 3.8: Shortest paths distribution



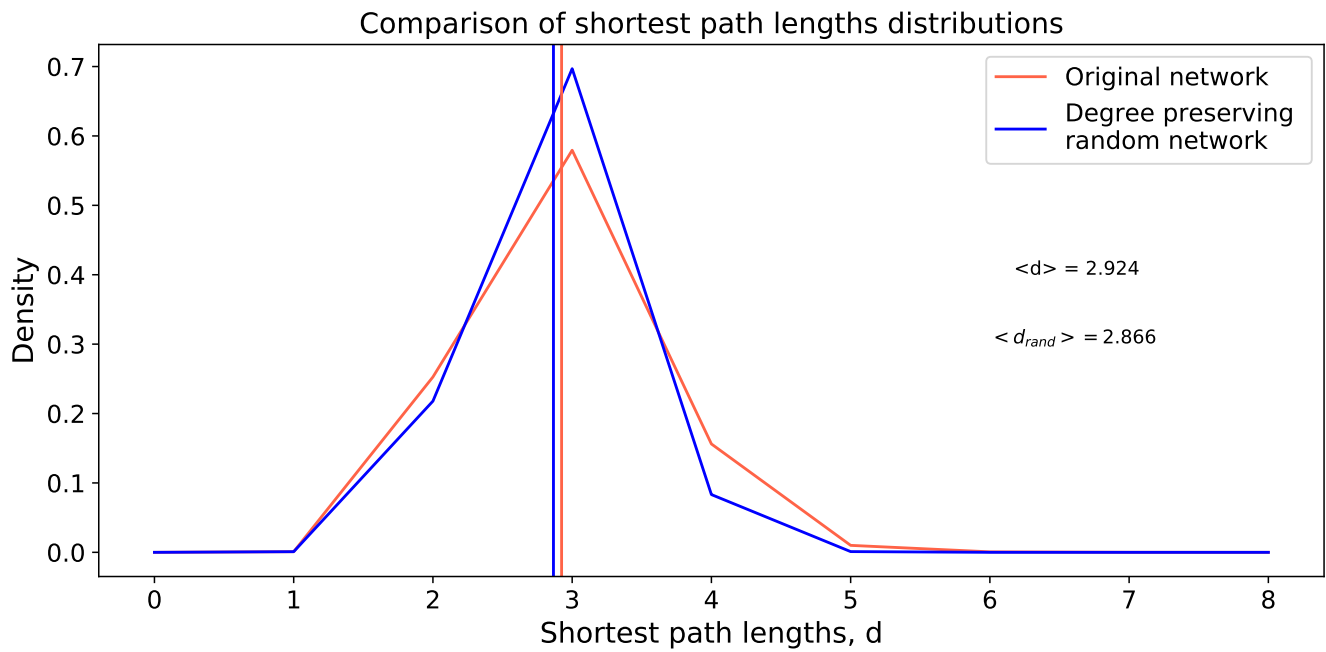


Figure 3.9: Shortest paths distributions comparison between the original largest connected component and a random network with degree preservation.

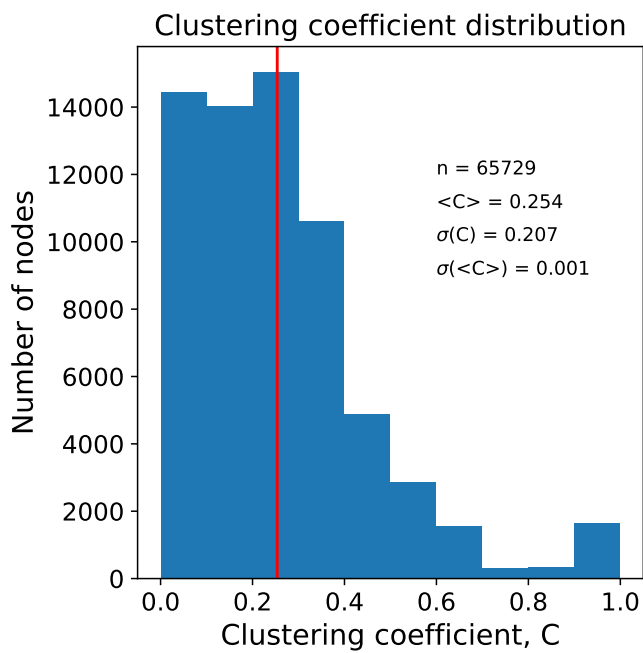


Figure 3.10: Clustering coefficient distribution

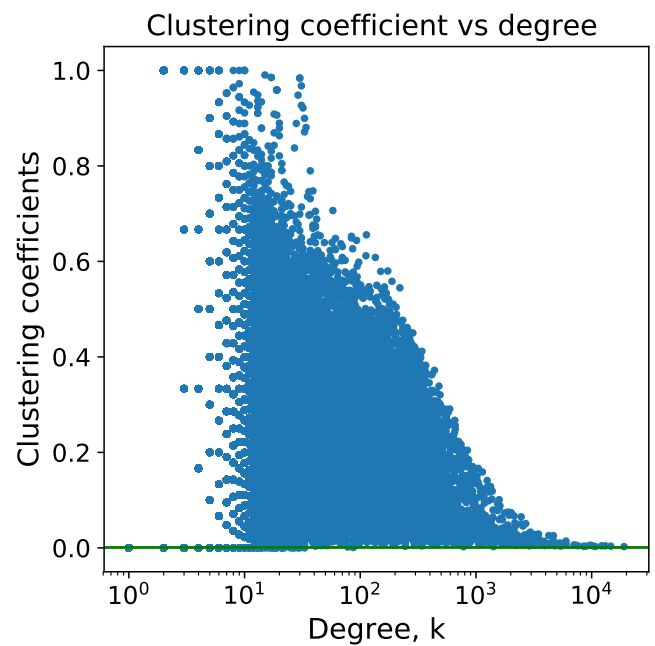


Figure 3.11: Clustering coefficients as function of the degree

### 3.3 Hubs analysis

The hubs of the crawled social network of tweets authors about the Cambridge Analytica-Facebook scandal are mainly news mass media, as expected. In Fig. 3.12 the 30 biggest hubs are represented by indicating the in-degree of the crawled network, corresponding to the number of authors following the hub, versus the actual total number of followers on Twitter. The "The New York Times" is the biggest hub, with the maximum number of both in-degree and number of followers. We observe that there is an obvious positive correlation between in-degree and followers, with some variations. In particular, let's take a pair of hubs having similar followers count, such as the "Washington Post" and the "Huffington Post". The "Washington Post" has a larger in-degree than the second. This difference can be interpreted as a larger interest in the scandal from the people following the "Washington Post" respect to the ones following the "Huffington Post". We can define a quantity to measure this interest:

$$\text{Interest} \equiv \frac{\text{in-degree}}{\# \text{followers}} \quad (3.4)$$

This measure represents the percentage of followers that being interested in the scandal had published a tweet about the subject.

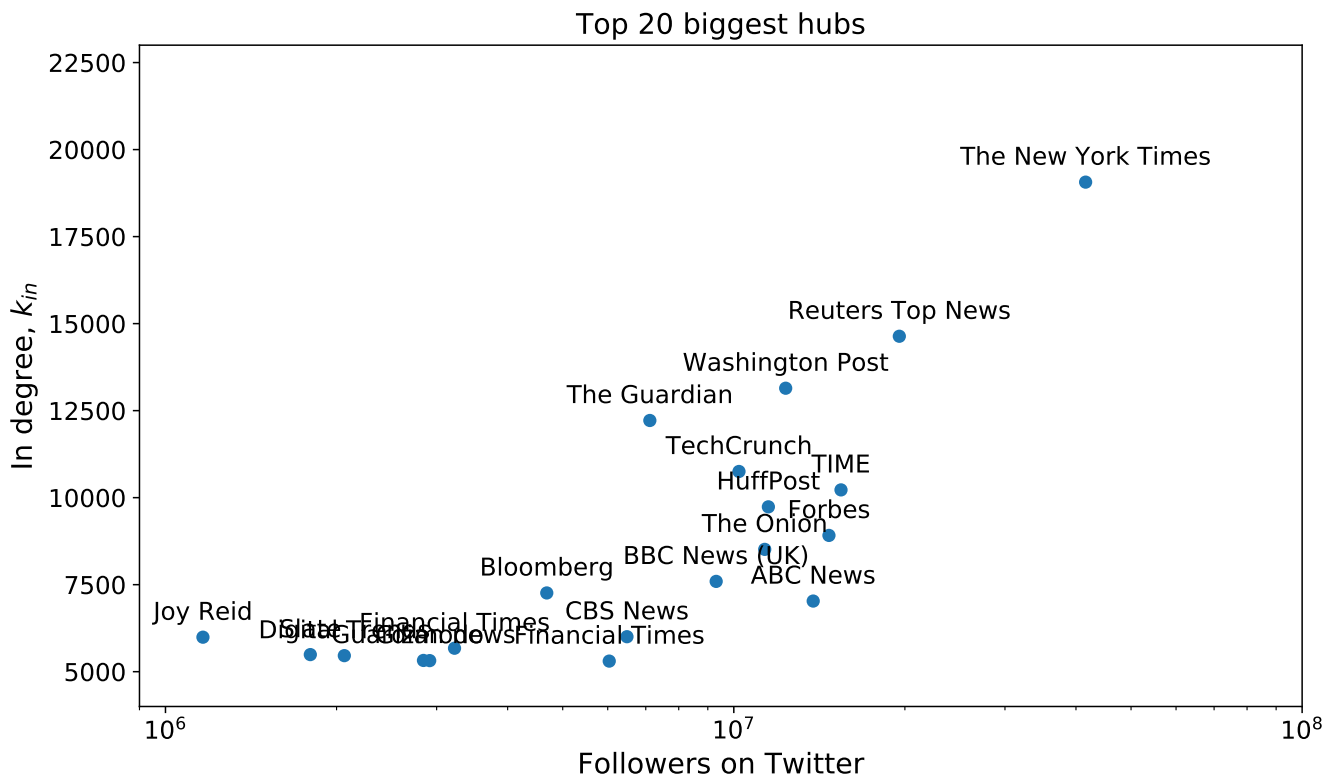


Figure 3.12

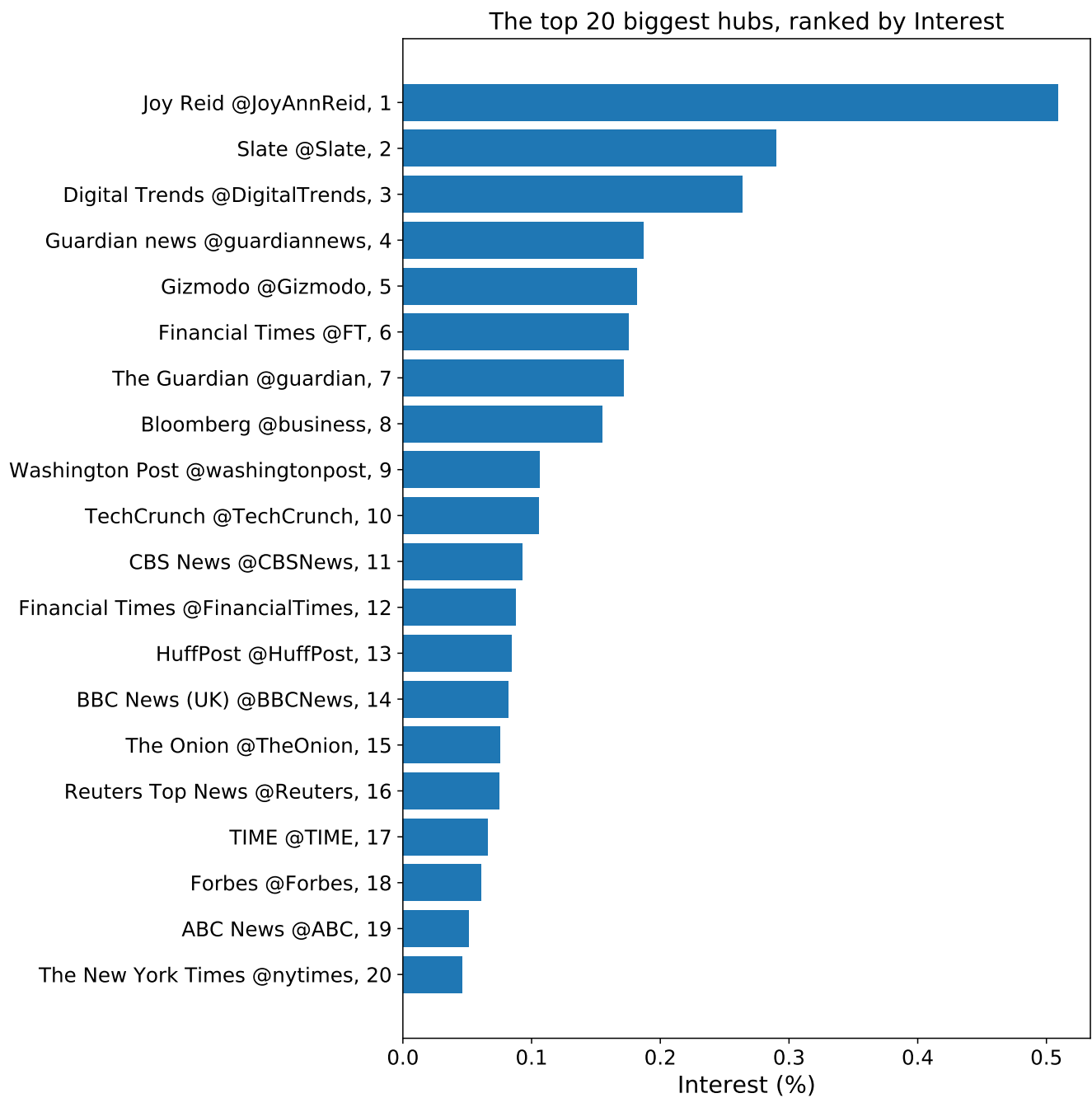


Figure 3.13

## 4 | Network dynamics

## 5 | Communities discovery

In this chapter we'll provide the results obtained by applying **K-Clique**, **Label Propagation**, **Louvain**, **Girvan-Newman** and **Demon** to a sample of 1000 nodes taken from the original network. We've chosen to sample the crawled data in order to ease the application of the various algorithms. Each partition is evaluated by applying an implementation of the scoring functions listed in [4], and, for each algorithm, the results are represented in a table. Together with the results of the scoring functions are also provided the total number of communities discovered (Communities), the number of nodes in the smallest/biggest community (Smallest/Biggest), the hashtags utilized in the biggest community (Tags) and finally the languages of the users in the biggest community (Langs).

### 5.1 K-Clique

We have chosen to apply the **K-Clique** algorithm, described in [5], to the sample using three different values for  $k$ : 3, 4 and 5, respectively. The results are represented in Table 5.1. As we can see, even if the result is not so good, the best partition is obtained by using  $k$  equals to 3, which returns a low modularity partition composed by low degree nodes. It is interesting to note that all the biggest partitions returned by the various applications of the algorithm are composed only by english speaking users.

K	Communities	Biggest	Smallest	Modularity	Conductance	IED	AND	Tags	Langs
3	21	30	3	0.12	0.56	0.21	2.51	cambridgeanalytica, deletefacebook, facebook, facebookgate	English
4	1	16	16	0.013	0.35	0.11	6.38	cambridgeanalytica, deletefacebook, facebook, facebookgate	English
5	2	7	6	0.00015	0.67	0.23	5.05	cambridgeanalytica, deletefacebook, facebook	English

Table 5.1: Evaluation of the partitions obtained by the application of the K-Clique algorithm.

### 5.2 Label Propagation

In Table 5.2 are represented the results of the application of the **Label Propagation** algorithm, described in [6]. According to the modularity score the partition provided by this algorithm represent a good subdivision of the original network, even if it is composed for the vast majority by small communities, as suggested by the high number of communities and the low value for the Average Node Degree score. As for the kclique algorithm, it is interesting to note that the biggest community is composed only by english speaking users.

Communities	Biggest	Smallest	Modularity	Conductance	IED	AND	Tags	Langs
714	53	1	0.65	0.26	0.18	1.48	zuckerberg, cambridgeanalytica, deletefacebook, facebook, facebookgate	English

Table 5.2: Evaluation of the partition obtained by the application of the Label Propagation algorithm.

### 5.3 Louvain

The application of the **Louvain**, described in [7], along with the last iteration of the Girvan-Newman algorithm, returns the best partition among all the partitions returned by the other algorithms. The results of its application are represented in Table 5.3. As for the Label Propagation algorithm, this partition also is composed by an high number of small communities, composed by nodes with degree between 1 and 2.

Communities	Biggest	Smallest	Modularity	Conductance	IED	AND	Tags	Langs
683	51	1	0.75	0.087	0.14	1.76	cambridgeanalytica, deletefacebook, facebook, facebookgate	English, Spanish

Table 5.3: Evaluation of the partition obtained by the application of the Louvain algorithm.

## 5.4 Girvan-Newman

For the **Girvan-Newman** algorithm, described in [8], we've decided to record the results of 5 iterations over the sample network. The results are represented in Table 5.4. As you can see, the first iteration returns a very poor partition, with a low modularity score, due to the fact that the edge with the highest betweenness centrality in the starting sample network doesn't provide a good grade of separation among the nodes of the network. With the second iteration, and the ones after that, there is a consistent improvement either in the modularity score and in the other measures.

Iteration	Communities	Biggest	Smallest	Modularity	Conductance	IED	AND	Tags	Langs
1	673	275	1	0.21	0.0049	0.20	1.40	cambridgeanalytica, deletefacebook, privacy, zuckerberg, facebook, facebookgate	English, French, Deutsch, Arabic, Spanish, Italian, Portuguese, Hindi, Finnish, Hungarian
2	674	165	1	0.55	0.011	0.19	1.49	cambridgeanalytica, deletefacebook, privacy, zuckerberg, facebook, facebookgate	English, French, Deutsch, Hindi, Finnish, Spanish
3	675	110	1	0.63	0.017	0.18	1.53	cambridgeanalytica, deletefacebook, privacy, zuckerberg, facebook, facebookgate	English, French, Deutsch, Arabic, Italian, Portuguese, Hungarian
4	676	110	1	0.66	0.025	0.17	1.57	cambridgeanalytica, deletefacebook, privacy, zuckerberg, facebook, facebookgate	English, French, Deutsch, Arabic, Italian, Portuguese, Hungarian
5	677	87	1	0.71	0.030	0.17	1.65	zuckerberg, cambridgeanalytica, deletefacebook, facebook, facebookgate	English, French, Deutsch, Italian, Hindi

Table 5.4: Evaluation of the partition obtained by the application of the Girvan-Newman algorithm.

In general, the partitions returned by the five iterations of the algorithms are all composed by an high number of small communities.

## 5.5 Demon

Finally in Table 5.5 we provide the results of the application of the **Demon** algorithm, described in [9], that we tested for three different values of  $\epsilon$ , 0.25, 0.50 and 0.75, respectively. In general, the three partitions are not so good from the point of view of the modularity score, with the first application of the algorithm beign the best among the three. Contrary to the results obtained by the application of the other algorithms, the partitions for the Demon algorithm are all composed by a small number of communities, with the last one being the "denser" one, which are composed by nodes with a degree between 3 and 4.

Epsilon	Communities	Biggest	Smallest	Modularity	Conductance	IED	AND	Tags	Langs
0.25	6	30	4	0.098	0.43	0.11	3.65	cambridgeanalytica, deletefacebook, facebook, facebookgate	English
0.50	9	30	4	0.085	0.49	0.12	4.05	cambridgeanalytica, deletefacebook, facebook, facebookgate	English
0.75	13	27	4	0.082	0.51	0.14	3.86	cambridgeanalytica, deletefacebook, facebook, facebookgate	English

Table 5.5: Evaluation of the partition obtained by the application of the Demon algorithm.

## 5.6 Comparisons

In this final section of the chapter we compare the algorithms used so far by confronting the best instances among the iterations provided in the past sections. The comparisons are performed by using the NF1 score, as described in [10].

A1	A2	F1 mean	Ground Truth Communities	Identified Communities	Community Ratio	Ground Truth Matched	Node Coverage	NF1
K-Clique 3	Label Propagation	0.44	714.0	21.0	0.029	0.022	0.10	0.0076
K-Clique 3	Louvain	0.32	683.0	21.0	0.031	0.016	0.10	0.0027
K-Clique 3	Girvan-Newman 5	0.25	677.0	21.0	0.031	0.012	0.10	0.0011
K-Clique 3	Demon 0.25	0.92	6.0	21.0	3.5	1.0	1.44	0.24
Label Propagation	Louvain	0.96	683.0	714.0	1.05	1.0	1.0	0.92
Label Propagation	Girvan-Newman 5	0.95	677.0	714.0	1.06	1.0	1.0	0.90
Label Propagation	Demon 0.25	0.38	6.0	714.0	119.0	1.0	14.17	0.0032
Louvain	Girvan-Newman 5	0.99	677.0	683.0	1.01	1.0	1.0	0.98
Louvain	Demon 0.25	0.38	6.0	683.0	113.83	1.0	14.17	0.0033
Girvan-Newman 5	Demon 0.25	0.36	6.0	677.0	112.83	1.0	14.17	0.0032

Table 5.6: Comparisons among the best iterations of the algorithms utilized in this chapter.

In Table 5.6 we can see the comparisons among the best iterations of the algorithms utilized during the community discovery phase. As we can see, the best results are returned by the comparisons between the Label Propagation, Louvain and Girvan-Newman (fifth iteration) algorithms, since that, as we've seen in the past sections, they are in fact the best performing algorithms among the ones we've tested for the communities discovery.

## 6 | Spreading

### 6.1 Which model for news spreading?

In order to choose a model for the spreading of news or ideas it's necessary to point out what means in this field an infection, and to interpret the related quantities. A person "infected" by a news it's not a person just only reached by the news, but it's a person who participates to the spreading by communicating to its neighbours and potentially infect them. The decision to spread the information it's an individual choice, expressing the interest of the person to the news, and indicates the presence of a personal threshold of reaction related to the news or ideas. The threshold can also be influenced by the neighbourhood or the community membership.

In the epidemic models, such as the SI model, the coefficient  $\beta$  represents the rate of transmission of the infection and it is constant for the whole population, indicating the dependence on the properties of the pathogen.

In the news field  $\beta$  can be interpreted as an intrinsic power of transmission of the news. This power of transmission may be associated to the journalistic concept of *newsworthiness*, which includes all the characteristics that make a fact a worthy news. But the expanding phenomenon of *fake news* shows that the speed of diffusion it's not only related to the worthiness of an information. A recent paper published on Science [11] shows how false news on Twitter spread "significantly farther, faster, deeper, and more broadly than the truth in all categories of information". The authors of the paper tried to explain the faster speed of diffusion of the false news by its novelty and the conveying of strongest emotive reactions like surprise or disgust.

A news coverage is usually characterized also by a certain amount of time after which the news naturally "dies" out. This fact can be modeled with the SIS formulation where the people recover from the infection with a rate  $\mu$ . The coefficient  $\mu$ , likewise  $\beta$ , it's constant and in this case can represents the intrinsic property of a news to vanish, which makes the people stopping communicating about the news.

In order to include also the personal threshold reaction to a news would be necessary to use a more sophisticated model, MILLI

In this chapter we'll describe the results we obtained by applying the **SI**, **SIS**, **SIR**, and **Threshold** diffusion models both on the crawled data and on the synthetic graphs (Erdős-Rényi and Barabási-Albert) generated from the original one. In each section, a comparison between the three networks will be provided along with some details on the implementation of the tests of every model.

### 6.2 The New York Times vs La Repubblica

Idea: let's start with the same news, but two different nodes, there is a big difference in diffusion?  
Prevision: no, the difference it's minimal because of the presence of hubs.



## 6.3 SI model

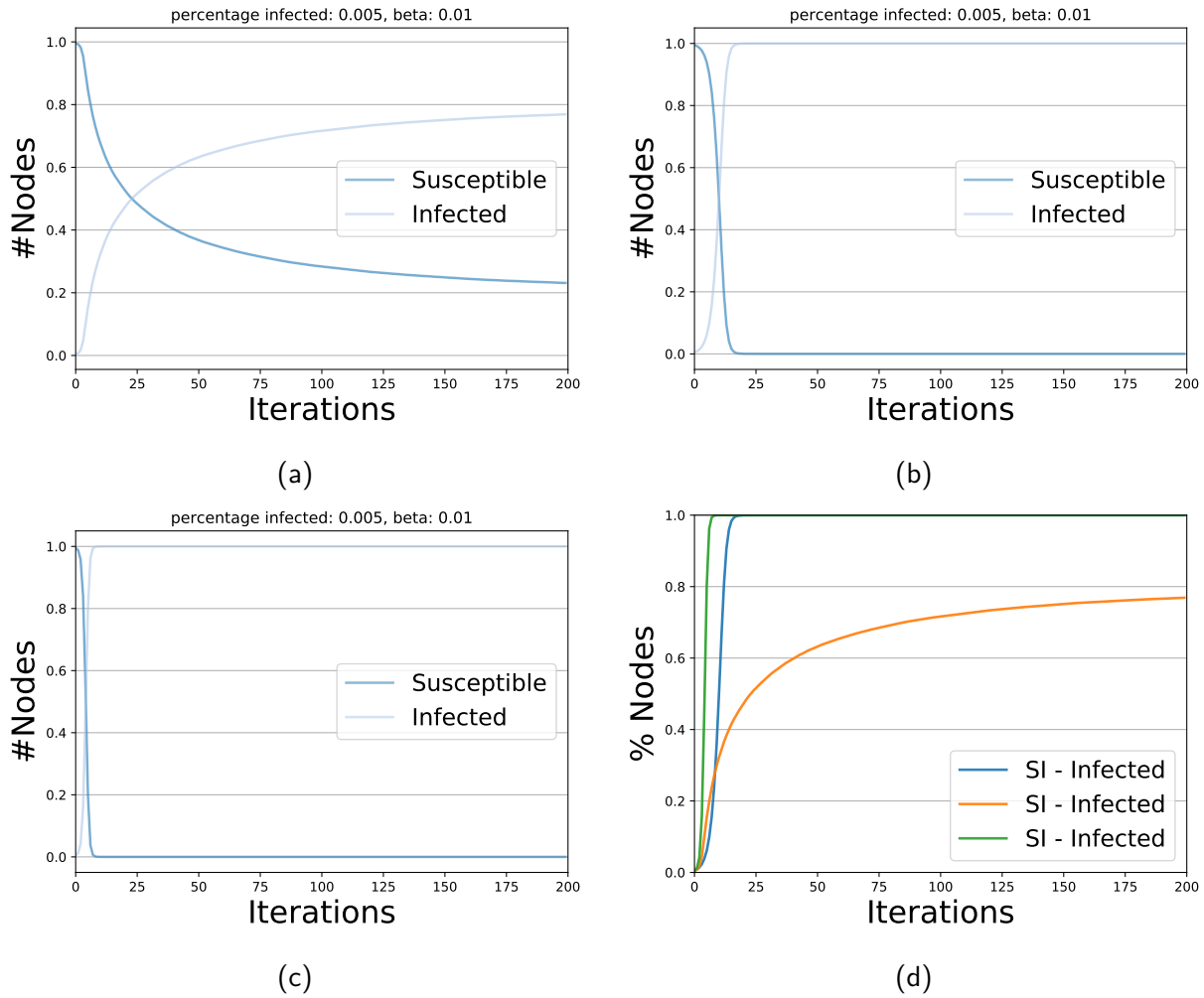


Figure 6.1: In Figure 6.1a we can see the diffusion graph for the original network, while in Figure 6.1b and in Figure 6.1c we can see the diffusion graph for the Erdős-Rényi and Barabási-Albert networks, respectively. In Figure 6.1d we can see a comparison between the infection rate of the three networks.

For the **Susceptible-Infected** model we've started with a 0.005% of the total population (3 nodes) of each network being infected, and we've chosen a value of 0.01 for the infection rate  $\beta$ . As you can see from Figure 6.1, the original network is the only one that doesn't reach the saturation regime, while the other networks reach it within the first 25 iterations of the model. This is due to the fact that both the Erdős-Rényi and the Barabási-Albert network are extremely connected, hence it is more easy for the infection to spread among the nodes.

## 6.4 SIS model

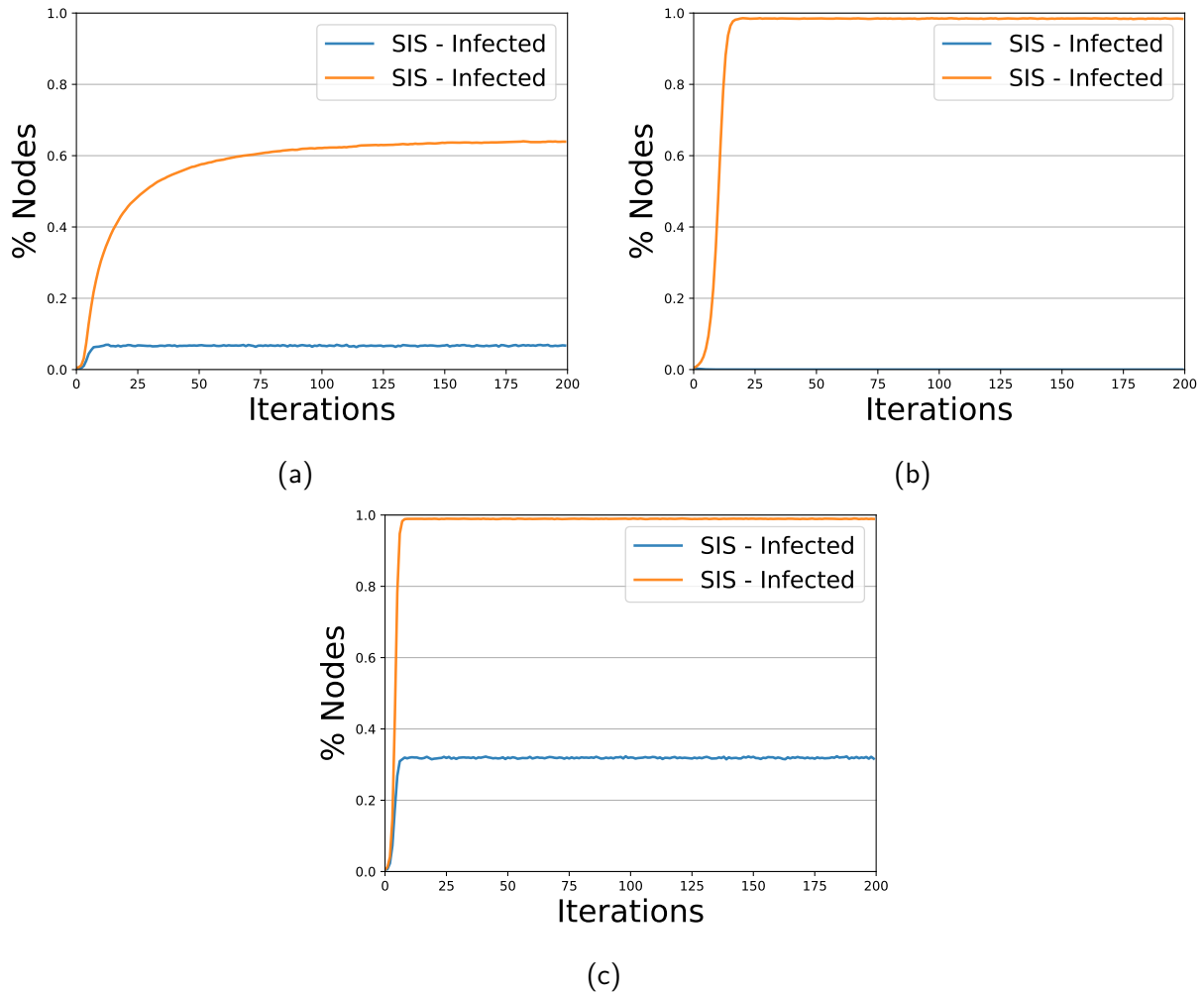


Figure 6.2: In Figure 6.2a we can see the comparison between the endemic state, in orange, and the disease free state, in blue, for the original network. The same comparison can be observed for the Erdős-Rényi and the Barabási-Albert network, respectively, in Figure 6.2b and 6.2c

For the **Susceptible-Infected-Susceptible** model, thanks to the introduction of the recovery rate  $\mu$ , we can model two possible outcomes for the epidemic: the **endemic state**, characterized by a low recovery rate and by the fraction of infected individuals that follows a logistic curve similar to the one observed for the SI model, for which  $\mu < \beta\langle k \rangle$ , and the **disease free state**, characterized by a sufficiently high recovery rate, for which  $\mu > \beta\langle k \rangle$ . A comparison between this two states is represented for every network in Figure 6.2.

## 6.5 SIR model

The key characteristic of the **Susceptible-Infected-Recovered** model consist in introducing the probability  $\gamma$  for the individuals to recover from the disease and hence to be "removed" from the population instead of returning to the susceptible state. We have chosen to test this model either for the case in which  $\gamma$  is smaller than  $\beta$  and the other way around. The graphs representing this different situations for all the three networks are visible in Figure 6.3.

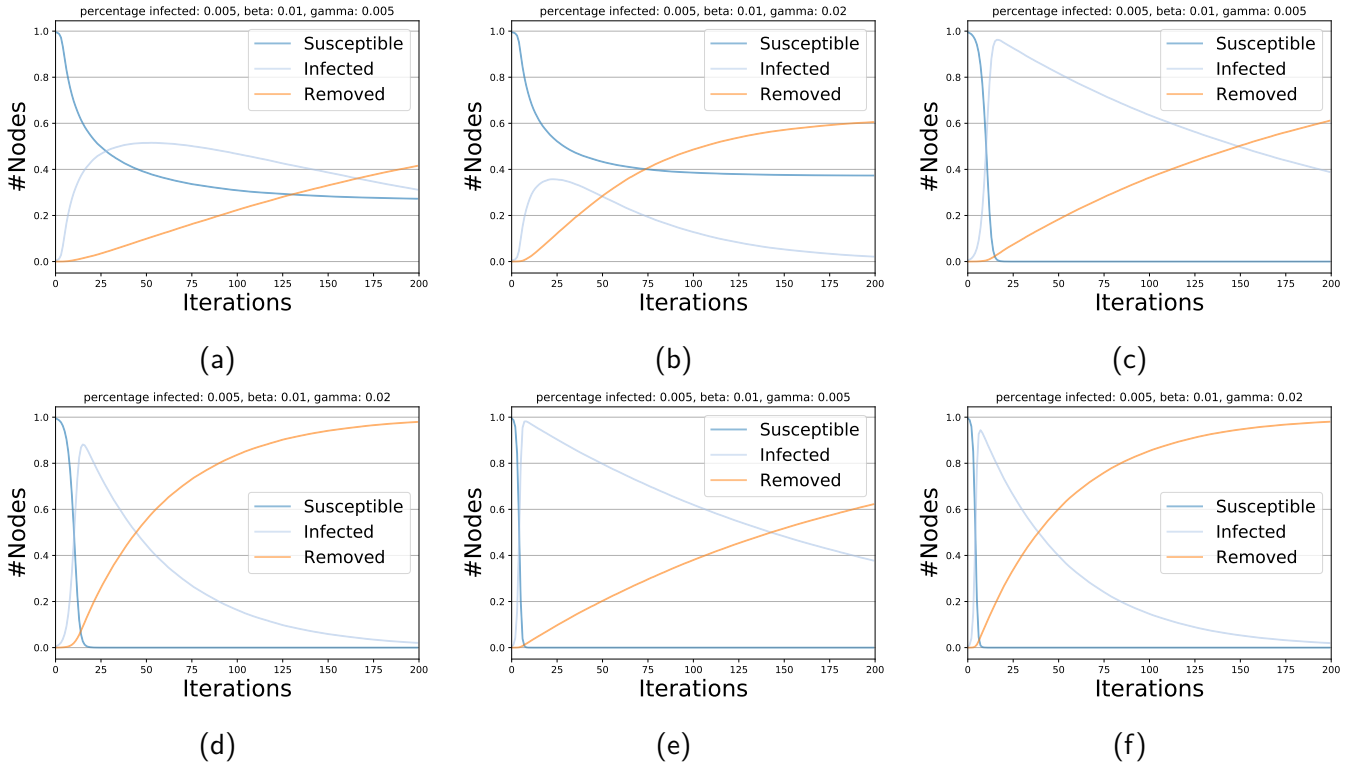


Figure 6.3: In Figure 6.3a and 6.3b we can see the representation of the diffusion on the original network both for the case in which  $\gamma$  is smaller than  $\beta$  and the other way around. The same kind of representation is plotted for the Erdős-Rényi network in Figure 6.3c and 6.3d and for the Barabási-Albert network in Figure 6.3e and 6.3f.

## 6.6 Threshold model

Finally we describe the application of the **Threshold model** both on the original network and the synthetic ones. In order to test this model we've chosen to apply a threshold  $\tau$  equals to 0.10, the diffusion of the infection for this model is represented in Figure 6.4. As we can see, for the original network we have that almost all the nodes become infected within the first 20 model's iterations, due to the fact that the value chosen for the threshold results to be sufficient for the spreading of the infection. If we change the threshold's value, this time using 0.20, we can observe that the original network become immune to the infection, thanks to its internal structure. We can observe the same immunity in the Erdős-Rényi and Barabási-Albert network for the original threshold's value.

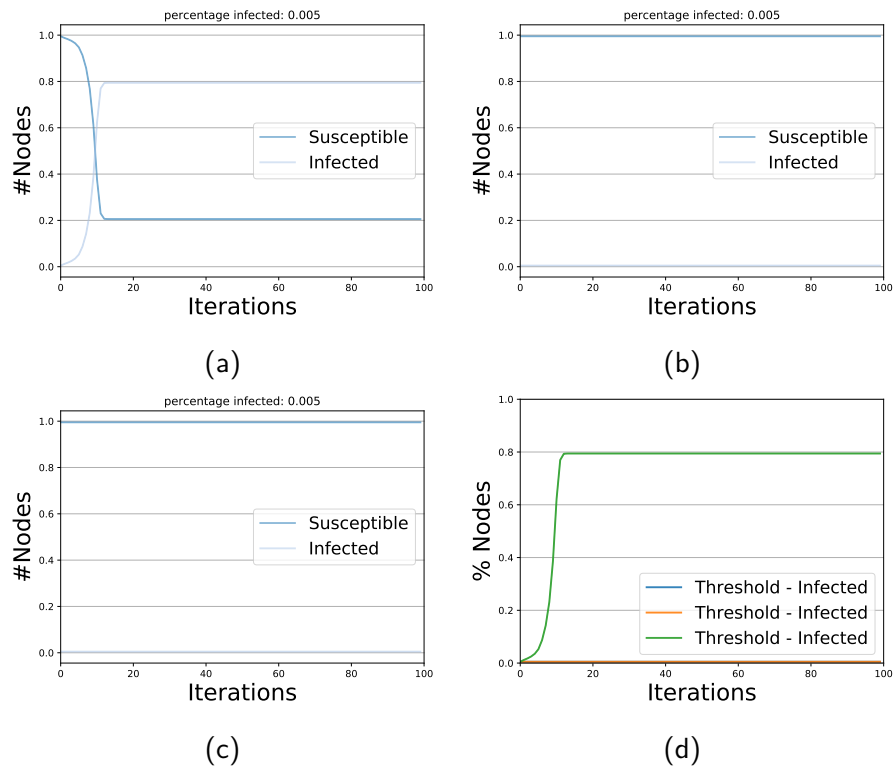


Figure 6.4: In Figure 6.4a is represented the diffusion of the infection for the original network, while in Figure 6.4b and 6.4c are represented the cases for the Erdős-Rényi and the Barabási-Albert network, respectively. A comparison between the three networks is represented in Figure 6.4d.

# 7 | Summary

# References

- [1] New York Times. *How Trump Consultants Exploited the Facebook Data of Millions*. <https://www.nytimes.com/2018/03/17/us/politics/cambridge-analytica-trump-campaign.html>. [Online; accessed 19-May-2018]. 2018.
- [2] New York Times. *Cambridge Analytica and Facebook: The Scandal and the Fallout So Far*. <https://www.nytimes.com/2018/04/04/us/politics/cambridge-analytica-scandal-fallout.html>. [Online; accessed 19-May-2018]. 2018.
- [3] Qi Ye, Bin Wu, and Bai Wang. "Distance Distribution and Average Shortest Path Length Estimation in Real-world Networks". In: *Proceedings of the 6th International Conference on Advanced Data Mining and Applications: Part I*. ADMA'10. Chongqing, China: Springer-Verlag, 2010, pp. 322–333. ISBN: 3-642-17315-2, 978-3-642-17315-8. URL: <http://dl.acm.org/citation.cfm?id=1947599.1947633>.
- [4] Yang Jaewon and Leskovec Jure. *Defining and Evaluating Network Communities based on Ground-truth*. <https://link.springer.com/article/10.1007/s10115-013-0693-z>. 2015.
- [5] Gergely Palla et al. *Uncovering the overlapping community structure of complex networks in nature and society*. <http://dx.doi.org/10.1038/nature03607>. 2005.
- [6] G. Cordasco and L. Gargano. *Community detection via semi-synchronous label propagation algorithms*. <https://ieeexplore.ieee.org/abstract/document/5730298/citations>. 2010.
- [7] Vincent D Blondel et al. *Fast unfolding of communities in large networks*. <http://stacks.iop.org/1742-5468/2008/i=10/a=P10008>. 2008.
- [8] M. Girvan and M. E. J. Newman. *Community structure in social and biological networks*. <http://www.pnas.org/content/99/12/7821>. 2002.
- [9] Michele Coscia et al. *DEMON: a Local-First Discovery Method for Overlapping Communities*. <http://arxiv.org/abs/1206.0629>. 2012.
- [10] Giulio Rossetti, Luca Pappalardo, and Salvatore Rinzivillo. *A Novel Approach to Evaluate Community Detection Algorithms on Ground Truth*. [https://doi.org/10.1007/978-3-319-30569-1\\_10](https://doi.org/10.1007/978-3-319-30569-1_10). 2016.
- [11] Soroush Vosoughi, Deb Roy, and Sinan Aral. "The spread of true and false news online". In: *Science* 359.6380 (2018), pp. 1146–1151. ISSN: 0036-8075. DOI: [10.1126/science.aap9559](https://doi.org/10.1126/science.aap9559). eprint: <http://science.sciencemag.org/content/359/6380/1146.full.pdf>. URL: <http://science.sciencemag.org/content/359/6380/1146>.